LA-7833-MS
Informal Report

Fireball Shape as a Height-of-Burst Diagnostic

LOS ALAMOS SCIENTIFIC LABORATORY
Post Office Box 1663 Los Alamos, New Mexico 87545

This report was not edited by the Technical Information staff.

Work supported by the Defense Nuclear Agency.

LA-7833-MS
Informal Report

Special Distribution
Issued: June 1979

Fireball Shape as a Height-of-Burst Diagnostic

Eric M. Jones
Jeffrey D. Colvin*

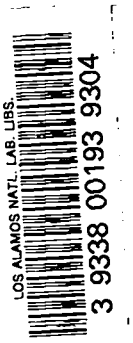

*EG&G, Inc., P.O. Box 809, Los Alamos, NM 87544.

FIREBALL SHAPE AS A HEIGHT-OF-BURST DIAGNOSTIC

by

Eric M. Jones and Jeffrey D. Colvin

ABSTRACT

The shock wave produced by an atmospheric nuclear fireball reflects from the ground and strikes the bottom of the glowing fireball at the time when the sum of the fireball radius and the shock radius equals twice the burst height. RADFLO calculations have been used to define the function R(fireball) + R(shock) = f(Y,t). Fireball shape information is used to determine the time when shock/fireball interaction occurs and to derive the height-of-burst.

I. INTRODUCTION

The evolution of an atmospheric nuclear fireball is governed by the weapon mass, yield and configuration, the pressure and temperature of the atmosphere, and the height-of-burst. In many military applications heights-of-burst are low enough that interaction between the glowing fireball and the shock wave reflected from the ground surface occurs long before buoyancy forces become important. In many of these applications, the desired effect is a sensitive function of burst height. Real-time height-of-burst data may be of potential value, particularly if the data can be determined from a single observing station.

Let us suppose that an atmospheric nuclear burst of unspecified yield occurs at an unknown range from a properly instrumented observing station. The parameters to be determined are yield, range, azimuth, and height-of-burst. We propose that all four parameters can be determined with two primary instruments and a small computer or processor. The two instruments are a bhangmeter and a fast read-out, "real-time" imaging array. The bhangmeter is used to determine minimum time and, hence, the yield while real-time fireball shape information provides the three remaining parameters.

II. METHOD

We presume that bursts of interest will be low-mass airbursts. The assumption of low mass assures that we will be dealing with weapons with high radiating temperatures and that the early fireball growth will be virtually spherical. U.S. atmospheric tests of weapons in massive towers or suspended from balloons show considerable asymmetries and brightness irregularities even at very late times. Air drops of low mass-to-yield ratios all produce very spherical fireballs.

The yield is determined from time-of-minimum measured with a bhangmeter.

During the blast wave phase of expansion the radius is closely approximated by

$$R = 301\ (Y/\rho)^{1/5}\ t^{2/5}, \tag{1}$$

where R is the radius in meters; Y the yield in kilotons; ρ the ambient atmospheric density in milligrams per cubic centimeter; and t the time in seconds. Because the radius is so insensitive to density it will probably be acceptable to assume a value for the density. An iterative scheme based on the as yet to be determined burst height could be adopted if deemed necessary.

Imaging data can be used to derive the time histories of the vertical and horizontal angular diameters. Knowledge of the yield and the horizontal angular diameter leads directly to the range and, from the position of the image on the detector, azimuthal data is obtained.

The final piece of data, the height-of-burst, can be obtained from comparison of the two angular diameters.

The fireball expansion will be spherical until the reflected shock wave strikes the glowing fireball. Shortly after shock/fireball interaction the bottom surface of the fireball is severely flattened. Before the interaction, the ratio of the vertical diameter to the horizontal diameter is approximately equal one but as the interaction proceeds the ratio drops sharply. Analysis of the time history of the diameter ratio provides a time-of-interaction which can then be used to derive the height-of-burst.

III. HEIGHT-OF-BURST SCALING DATA

The LASL one-dimensional, spherical, radiation transport/hydrodynamics program RADFLO has been very successful in calculating atmospheric nuclear fireball evolution. Fireball and shock radii produced by the program are in good agreement with data.

We assume with some confidence that the shock/fireball interaction occurs when

$$R_{SH} = 2H - R_{FB} \tag{2}$$

where R_{SH} is the shock radius, R_{FB} is the fireball radius and H is the burst height (Figure 1). We recognize that the reflected shock traverses slightly heated air before striking the fireball and that the interaction actually occurs slightly before the time given by equation (2). However, we expect that the effect is small compared to likely yield uncertainties.

A series of RADFLO calculations have been made for bursts of various yields at sea-level density (1.2×10^{-3} gcm^{-3}). The fireball radius was chosen as the 0.2 eV temperature contour while the shock radius was chosen as the location of maximum density in the computed shock profile. Positional uncertainties are about one cell width or about one percent of the radius. These data were used to compute time histories of $R_{SH} + R_{FB}$. The results are presented in figure 2.

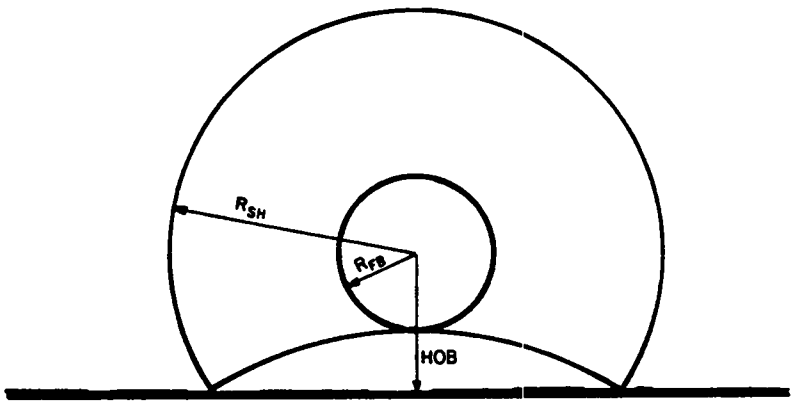

$$R_{FB} + R_{SH} = 2 \cdot HOB$$

Fig. 1

Determination of the time of fireball/shock interaction permits derivation of burst height.

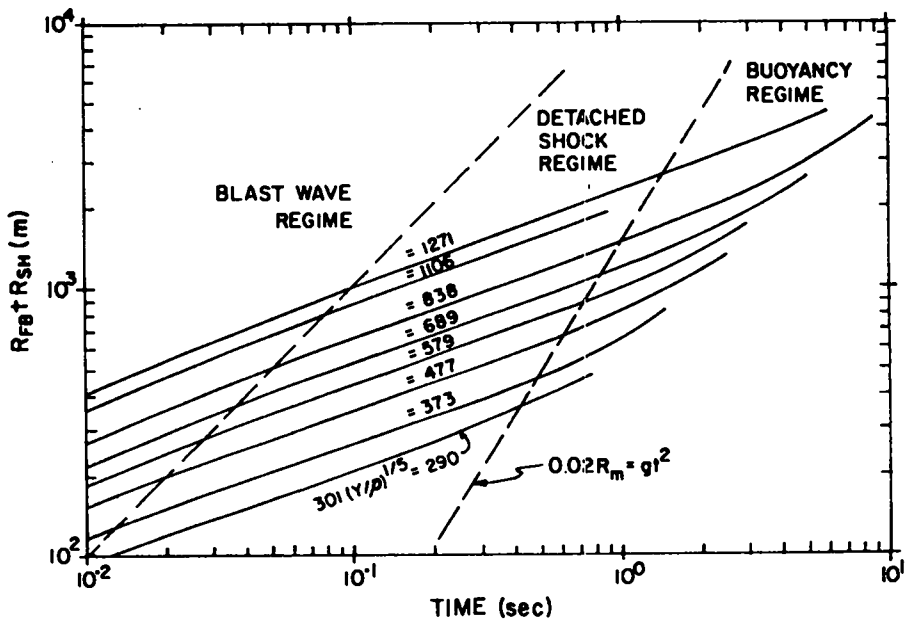

Fig. 2

The fireball radius (R_{FB}) and shock radius (R_{SH}) are calculated with RADFLO. Knowing the yield and time of fireball/shock interaction gives $2H = R_{FB}+R_{SH}$ from the graph. See the text for a further discussion of this figure.

The curves in figure 2 are labeled with the parameter 301 $(Y/\rho)^{1/5}$. The curves, in ascending order, correspond to sea-level bursts with yields of 1, 3.5, 12, 32, 75, 200, 800, and 1600 kilotons.

The plane of figure 2 is divided into three phenomenological regions. During the early fireball expansion the air immediately behind the shock has been heated to greater than 0.2 eV and the shock and fireball radii are identical. During this blast wave phase both radii are closely approximated by equation 1. At a time given by the leftmost dashed line, the weakened shock is no longer capable of heating air above 0.2 eV and the shock "detaches" from the fireball.

At very late time, fireballs which have not yet undergone shock interaction are deformed by buoyancy forces. The vertical deformation is approximately given by

$$\Delta R = gt^2 \qquad (3)$$

where $g = 9.8\ m\ s^{-2}$ is the gravitational acceleration. During the late fireball evolution the fireball radius reaches a maximum and slowly declines thereafter while the shock wave velocity approaches the sound speed. (The upward curvature of the $R_{FB} + R_{SH}$ lines is a result of this behavior.) The maximum fireball radius is designated as R_M. If the buoyant deformation exceeds a few percent, the height-of-burst analysis suddenly becomes more complex. This buoyancy regime has been delineated by the $\Delta R = 0.02\ R_M$ line at the right of figure 2.

The graph is used as follows: the time of shock/fireball interaction is determined from the history of the ratio of the vertical to horizontal diameters. The known yield is then used to interpolate between the curves and the burst height is read as half the sum of the two radii.

IV. TEST DATA

We have analysed photographic data for seven U.S. atmospheric nuclear tests conducted in Nevada for which unclassified yields are available and one Pacific test. All were low mass air drops. The relevant data for the seven events with the unclassified yields are given in Table I. All had $\rho = 1.0 \times 10^{-3}$

gcm^{-3}. The histories of the ratio of the vertical and horizontal diameters are given in figures 3 through 9. For the purpose of this paper we have merely estimated the interaction time as the time of a significant, sustained drop of the diameter ratio. The range of the estimated interaction time (t_i) for each event is given in Table I.

The derived burst heights (H_D) are plotted against the actual heights in figure 10. Clearly, the errors are less than 50 meters in all cases. The relative errors are given in Table I for the seven unclassified events. All eight events have errors less than 20 percent.

TABLE I

THE SEVEN NTS AIR DROP EVENTS EXAMINED IN THIS STUDY

NAME	$\frac{Y}{(kt)}$	$\frac{H}{(m)}$	$\frac{H/Y^{1/3}}{}$	$\frac{t_i}{(s)}$	$\frac{301(Y/\rho)^{0.2}}{(ms^{-0.4})}$	$\frac{H_D}{(m)}$	$\frac{H_D-H}{H}$
GRABLE	15	160	65	.075-.1	518	180	.13
FIZEAU	11.4	152	68	.08-.1	490	180	.18
CLIMAX	62.8	407	102	.3-.45	689	415	.02
TS-DOG	19	317	119	.4-.5	543	350	.10
BJ-EASY	31	401	128	.3-.5	599	368	-.08
BJ-CHARLIE	14	345	143	.45-.5	511	328	-.05
WASP-PRIME	3	222	157	.4-.5	375	224	-.01

V. REFINEMENTS

This simplistic discussion of shock/fireball interactions has led to fairly accurate burst height estimation for eight nuclear tests. Some fine tuning of the model may improve the results and/or indicate presently unidentified limitations.

1) For bursts which suffer ground interaction before minimum time, t_{MIN} is a function of burst height. Calculational work has been done to define the variation with height for a series of bursts with the IVY-KING yield (540 kt). These results are plotted in Figure 11. The analysis routines for determining burst height should include an iterative scheme to account for modified yield estimates at low burst heights.

2) Numerical tests of existing photographic data must be made to determine the effects of finite resolution elements and threshold sensitivities on the results. We imagine that there is a tradeoff between fine resolution and accurate diameter ratio measurements on the one hand and reduced integration times with coarse grids on the other. We intend to perform computer simulations of selected data frames to quantify these effects, and to determine the limitations imposed by the frame time resolution of typical imaging devices ($\sim$ 1/30 s).

3) Similarly, atmospheric attenuation and decreasing intensities with increasing range may introduce errors. Fireballs which suffer interaction after a few times second-maximum do not have particularly well defined edges. Unless properly treated, range and height-of-burst errors may be introduced which are, themselves, functions of range.

4) The speed of deformation during the early stages of the interaction is a function of yield and height-of-burst. Analysis of this motion may provide an independent burst height indicator although we anticipate that it will not be particularly sensitive. Definition of scaling laws will require analysis of two-dimensional calculations.

Figure 12 represents the analysis flow in a hypothetical system including an iterative consideration of the effects of height-of-burst on t_{MIN}. We are currently implementing such an analysis scheme to test the validity of this height-of-burst determination technique.

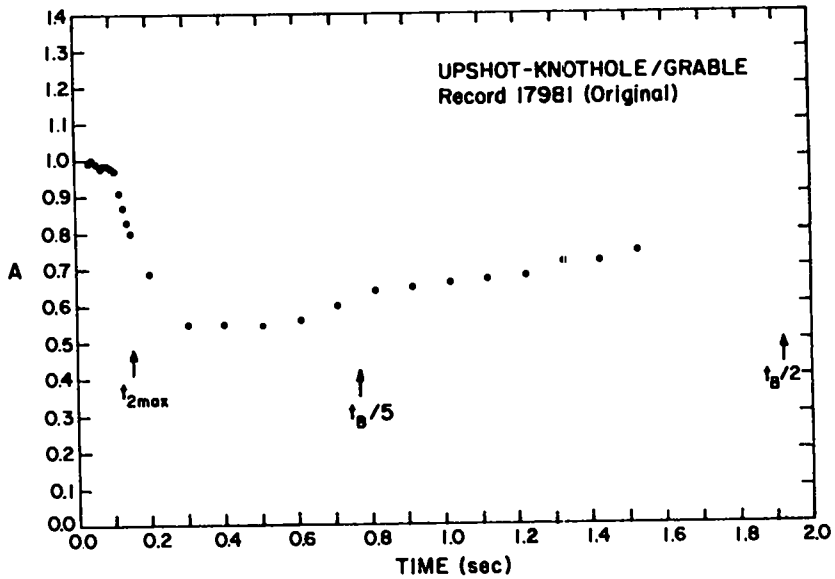

Fig. 3

Ratio of the vertical to the horizontal diameter as a function of time for GRABLE. GRABLE was a 15 kt explosion 160 m above the ground surface at the Nevada Test Site (NTS). t_{2MAX} is the calculated time of second thermal maximum while t_B, the buoyancy time, is given by $R(t_{2MAX}) = g\, t_B^2$. Examination of the GRABLE photographs shows initial interaction at about 0.07 s although no substantial deformation occurs until about 0.1 s.

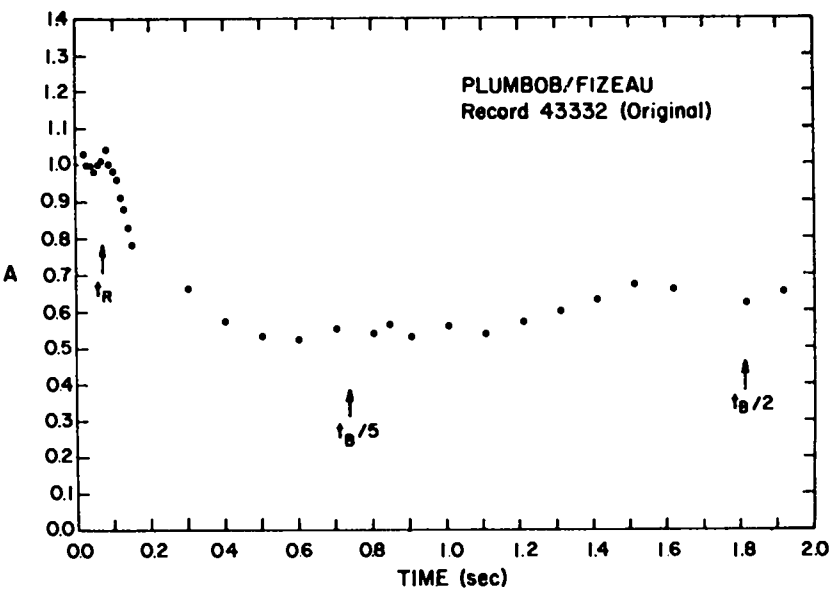

Fig. 4

FIZEAU was a 11.4 kt explosion at 152 meters. t_R is the time of initial interaction determined from visual inspection of the photographic records.

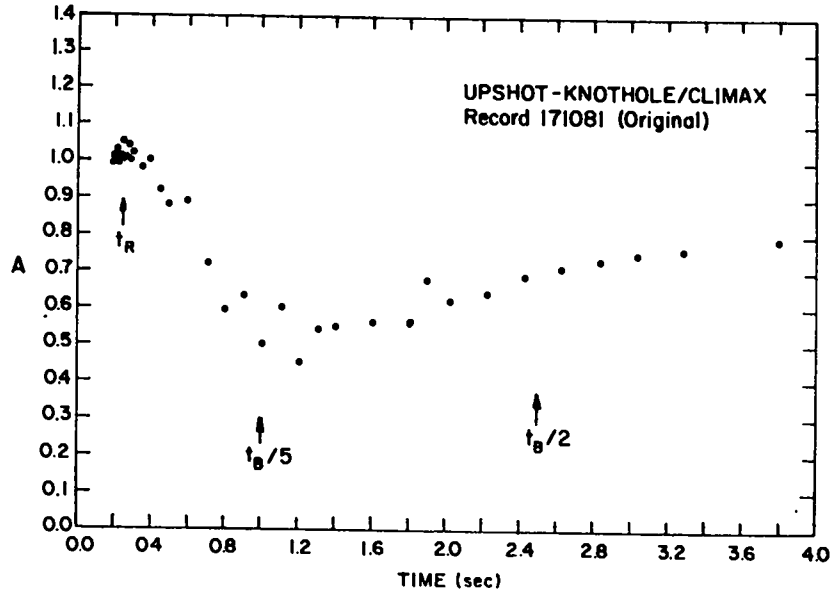

Fig. 5

CLIMAX was a 63 kt explosion at 407 m burst height.

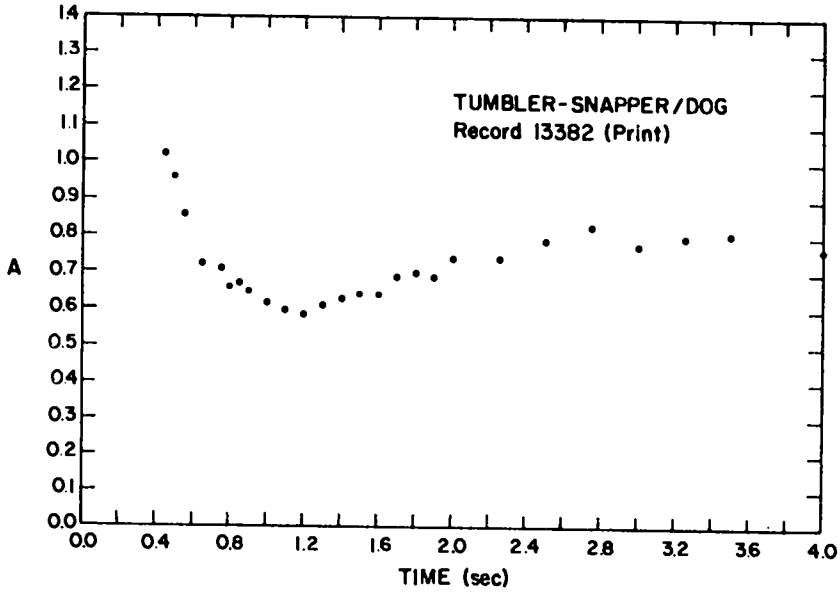

Fig. 6

TS-DOG was 19 kt explosion at 317 m burst height.

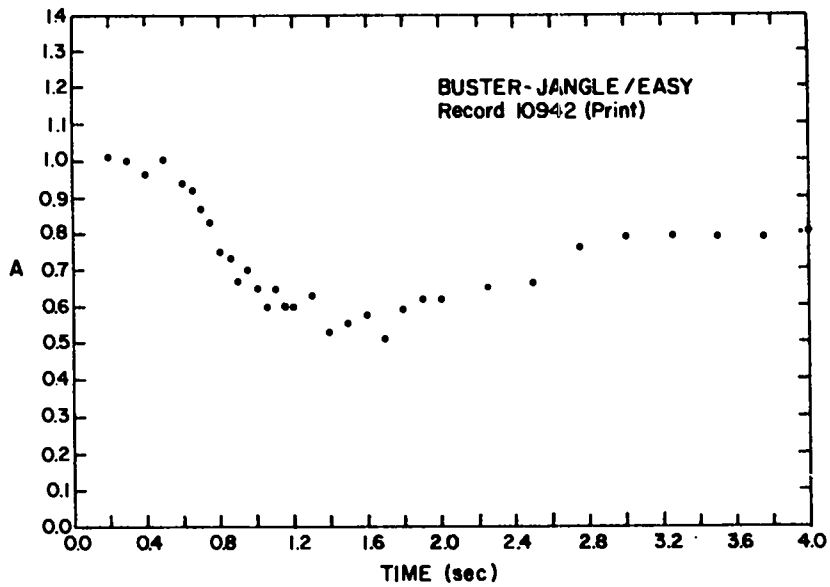

Fig. 7

BJ-EASY was a 31 kt explosion at 401 m.

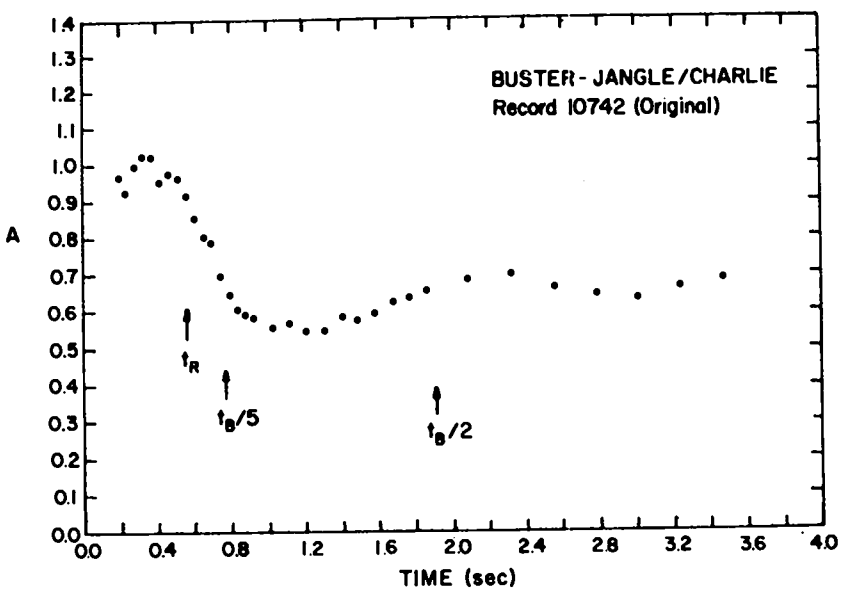

Fig. 8

BJ-CHARLIE was a 14 kt explosion at 345 meters burst height.

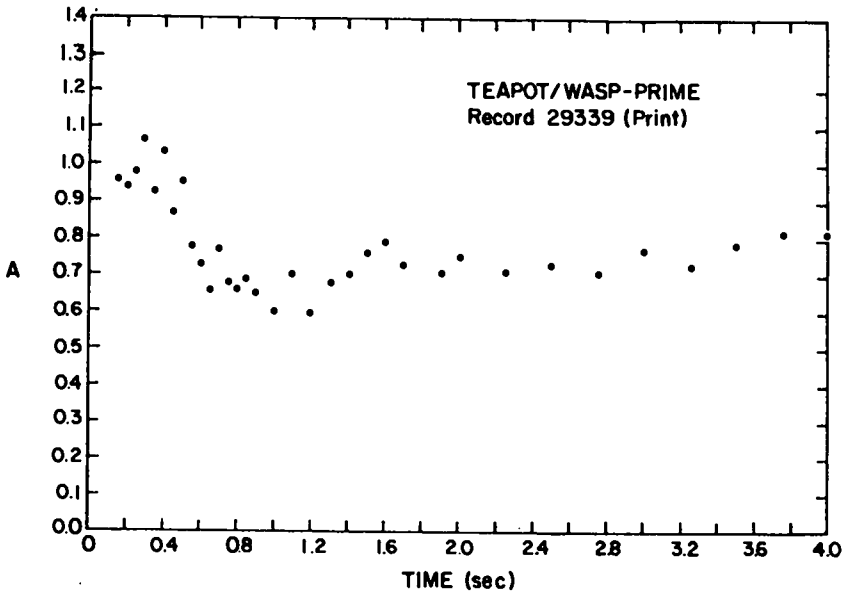

Fig. 9

WASP PRIME was a 3 kt explosion at 222 m burst height.

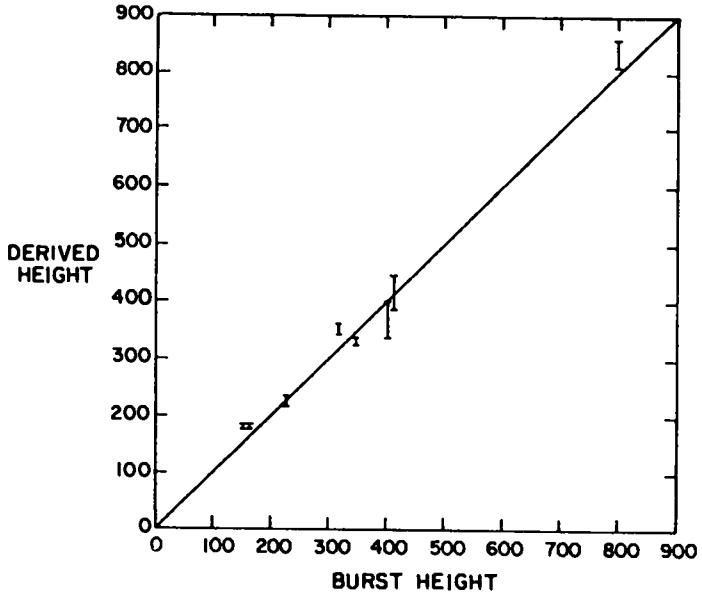

Fig. 10

For each of the seven Nevada test studied and one Pacific Test (DOMINIC AZTEC) the derived heights agree well with the actual heights. The range for each test indicated the height uncertainty produced by the uncertainty in the time of interaction.

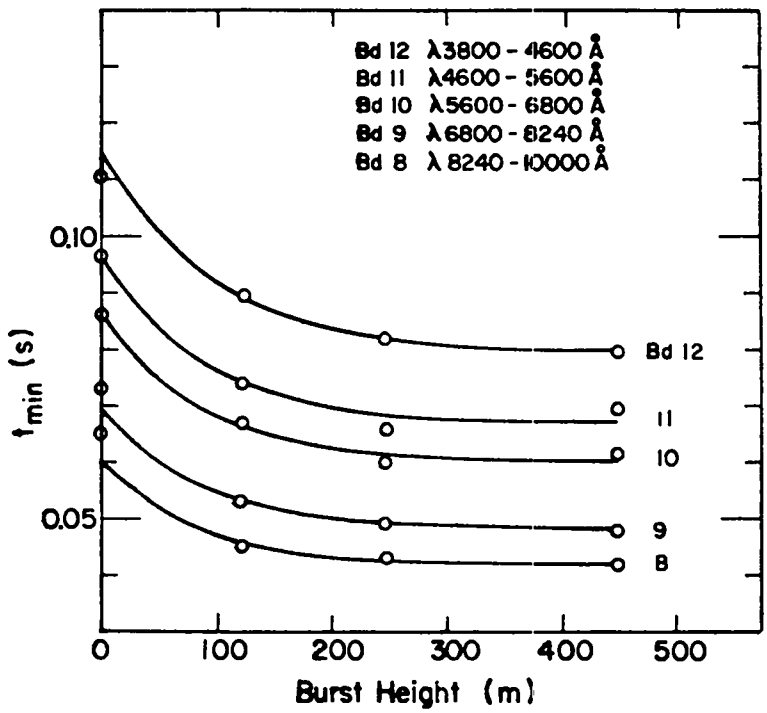

Fig. 11

Time of thermal minimum (t_{MIN}) in various wavelength bands calculated for 540 kiloton explosions at various altitudes.

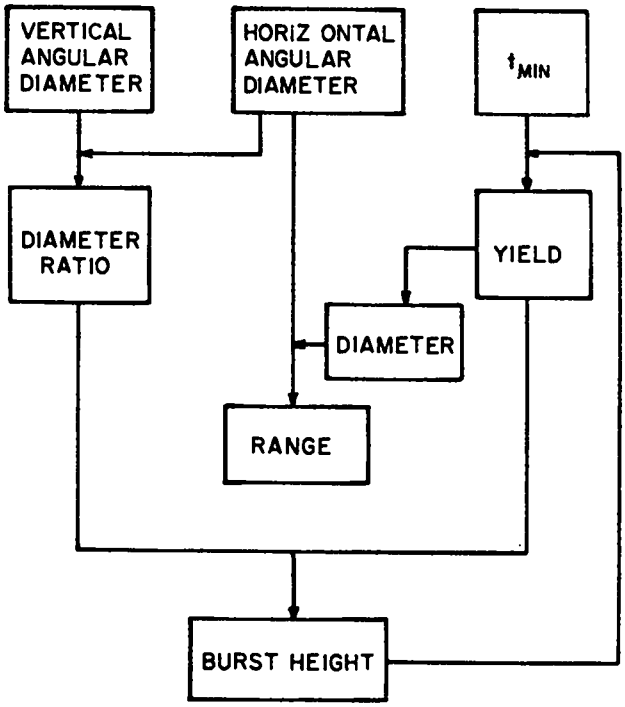

Fig. 12

A simplified block diagram of an analysis routine to determine burst height. The top three boxes contain data input into the analysis routine. Minimum time provides an initial yield estimate which may require modification due to burst height effects.